Heat Mass Transfer (2017) 53:2829–2839
DOI 10.1007/s00231-017-2006-7

ORIGINAL

Influence of heat conducting substrates on explosive crystallization in thin layers

Wilhelm Schneider[1]

Received: 10 December 2016 / Accepted: 28 February 2017 / Published online: 28 March 2017

Abstract Crystallization in a thin, initially amorphous layer is considered. The layer is in thermal contact with a substrate of very large dimensions. The energy equation of the layer contains source and sink terms. The source term is due to liberation of latent heat in the crystallization process, while the sink term is due to conduction of heat into the substrate. To determine the latter, the heat diffusion equation for the substrate is solved by applying Duhamel's integral. Thus, the energy equation of the layer becomes a heat diffusion equation with a time integral as an additional term. The latter term indicates that the heat loss due to the substrate depends on the history of the process. To complete the set of equations, the crystallization process is described by a rate equation for the degree of crystallization. The governing equations are then transformed to a moving co-ordinate system in order to analyze crystallization waves that propagate with invariant properties. Dual solutions are found by an asymptotic expansion for large activation energies of molecular diffusion. By introducing suitable variables, the results can be presented in a universal form that comprises the influence of all non-dimensional parameters that govern the process. Of particular interest for applications is the prediction of a critical heat loss parameter for the existence of crystallization waves with invariant properties.

Dedicated to Professor W. Linzer on the Occasion of his 80th Birthday.

✉ Wilhelm Schneider
wilhelm.schneider@tuwien.ac.at

[1] Institute of Fluid Mechanics and Heat Transfer, Technical University of Vienna, Vienna, Austria

1 Introduction

When a short heat pulse is applied to an amorphous material, e.g. by a line laser, causing the temperature to rise locally well above the glass transition temperature of the material, crystallization sets in. The process of crystallization is associated with the liberation of the latent heat of fusion. The conduction of heat then gives rise to a temperature increase near the site of the heat pulse, thereby causing further crystallization. Under certain conditions, which are the main topic of the present work, this process may lead to a self-sustaining crystallization front that is propagating through the material. Depending on the material, the propagation velocity can be quite large, justifying the common use of the technical term "explosive crystallization" for the process. In amorphous germanium, for instance, crystallization fronts have been observed propagating with velocities of the order of several meters per second [1]. In polymers, however, only very small propagation velocities can be expected. For polypropylene, propagation velocities between 3 nm/s and 0.3 mm/s have been predicted [2]. For a survey of the pertinent literature, one may consult the recent paper [3].

In many applications of engineering interest, explosive crystallization takes place in a thin film that is mounted on a substrate, with the crystallization front propagating in a direction parallel to the film surface. A theoretical description of the process requires the solution of two main problems. The first one concerns the kinetics of non-isothermal crystallization, the second one consists in determining the heat loss from the crystallizing layer to the heat conducting substrate. Apparently, the first analysis of self-sustaining crystallization fronts based on rate equations for crystallization [4] has been presented in [5] and published in [2, 6]. The related problem of stationary crystallization fronts in continuous crystallization was considered in [7]. Those theoretical investigations were restricted to adiabatic processes. With regard to heat losses, it was shown in [3, 8–10] that a local formulation, such as an effective heat transfer coefficient, is insufficient for describing the effect of heat conduction into the substrate. For a crystallization wave that propagates with invariant properties, the classical solution of a moving heat source was applied and an integro-differential equation for the temperature distribution in the crystallizing layer was obtained [3, 8–10]. Together with one [8, 9] or more [3, 10] rate equations, the integro-differential equation gives a complete set of equations of an eigenvalue problem, with the unknown propagation velocity as the eigenvalue.

In [3, 8–10] the eigenvalue problem was solved numerically, which is a bit cumbersome owing to the integro-differential equation. Results were obtained that are of interest from a theoretical point of view as well as with respect to applications. Among others, a critical value of a non-dimensional parameter characterizing the heat loss was found in [8, 9], leading to dual solutions below the critical value and a lack of solutions above. However, the results were obtained only for a particular set of a rather large number of non-dimensional parameters. With another parameter set [3, 10], the critical behaviour with respect to the heat loss was confirmed, but numerical difficulties did not allow to obtain more than a small fraction of a second branch of the solution.

In view of both numerical difficulties and uncertainties associated with conclusions based solely on particular parameter sets, it is helpful to observe that analytical solutions were obtained in [2, 5, 6] for the adiabatic case by applying the method of matched asymptotic expansions for very large activation energies. The great advantages of analytical vs. numerical solutions provides the motivation for the present work, which aims at obtaining analytical solutions for explosive crystallization in thin layers subject to heat losses due to the presence of a heat conducting substrate. In addition, more general governing equations will be presented to allow the prediction of arbitrary time-dependent crystallization processes, i.e., without restriction to waves of invariant properties.

2 Formulation of the problem

The formulation of the problem follows [8, 9], with some modifications. As shown in Fig. 1, the process of explosive crystallization is modeled as a crystallization zone that moves into an initially amorphous layer of constant thickness δ_L. Behind the crystallization zone the volume fraction of the crystalline phase, briefly addressed as degree of crystallization, ξ, approaches asymptotically

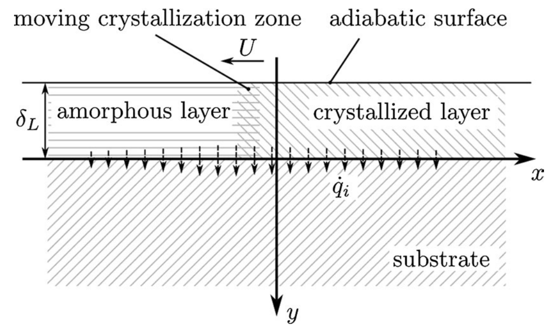

Fig. 1 Sketch of the explosive-crystallization process [8]

the value $\xi = 1$ for fully completed crystallization. It is assumed that the process is two-dimensional, i.e. depending only on the Cartesian coordinates x and y, and on time t. This is in accord with certain, though not all, experiments, e.g. [11, 12]. The crystallizing layer (briefly addressed as "layer" in what follows) is mounted on a heat conducting substrate, whose extent in y-direction is much larger than the thickness of the layer. Thus the substrate may be considered as a semi-infinite body, whose temperature at infinity is equal to the initial temperature of the substrate, T_S. All thermo-physical properties of the layer and the substrate are assumed to be constant, i.e. independent of the temperature and, in case of the layer, also independent of the degree of crystallization.

Latent heat is liberated in the course of the crystallization process, giving rise to a temperature increase. If the layer were adiabatic, the temperature would rise asymptotically to the temperature

$$T_{\text{ad}} = T_S + \frac{l}{c_{pL}} \tag{1}$$

behind the crystallization zone, where l is the specific latent heat of fusion, while c_{pL} is the isobaric specific heat capacity of the layer.[1] However, due to heat conduction from the layer into the substrate there is a heat flux $\dot{q}_i$ at the interface that acts as a heat loss to the layer. In the present investigation, the thermal contact between the layer and the substrate is assumed to be sufficiently good to justify disregarding any contact resistance; but see [3, 10] for the effect of a small contact resistance. Very far from the crystallization zone thermal equilibrium between the layer and the substrate is established, i.e. the temperature of the layer approaches T_S as $x \to \pm\infty$.

[1] In case of polymers, there is a maximum volume fraction of the crystalline phase, V_∞. The degree of crystallization, ξ, is then defined as the crystalline volume fraction referred to its maximum value, while l is to be multiplied by V_∞ to obtain an effective specific latent heat [8].

3 Basic equations for the thin crystallizing layer

3.1 Energy equation

It is a classical approach to describe heat conduction in a thin layer in a one-dimensional approximation. In the present case, however, providing an a priory justification for the one-dimensional approximation is not straightforward. The problem is discussed in [3], with the conclusion that the use of the one-dimensional approximation for the heat conduction in the layer appears to be justified for explosive crystallization under common conditions. The energy balance for the crystallizing layer then reduces to the equation

$$\frac{\partial \Theta}{\partial t} - \alpha_L \frac{\partial^2 \Theta}{\partial x^2} = \frac{\partial \xi}{\partial t} - \frac{\dot{q}_i}{\delta_L \varrho_L l} \tag{2}$$

for the non-dimensional temperature difference

$$\Theta = \frac{T - T_S}{T_{\mathrm{ad}} - T_S} = \frac{c_{pL}(T - T_S)}{l}, \tag{3}$$

with α_L as the thermal diffusivity of the layer and ϱ_L as the density of the layer. On the right-hand side of the heat diffusion Eq. (2) there is a source term due to the local liberation of the latent heat and a sink term due to the interface heat flux. Heat losses at the free surface of the layer are neglected. The source term is proportional to the crystallization rate, $\partial \xi / \partial t$, which is to be determined from one or more rate equations that follow from the kinetics of crystallization.

3.2 Rate equation of crystallization

According to [4], a non-isothermal crystallization process can be described by a system of rate equations. Originally, the system of rate equations was derived on the basis of the crystallization theory developed in [13–16] for heterogeneous crystallization. Later, an analogous system of rate equations was given also for homogeneous crystallization [3, 10]. The application to crystallization processes requires numerical solutions [3, 10]. Since the main purpose of the present analysis is to provide a better understanding of the effect of the substrate, it appears sufficient to describe the kinetics of crystallization in the simplest possible way, i.e. for the limiting case of very large activation rate of nuclei as compared to their growth rate [4]. This leads to the following single rate equation as already applied in [8, 9]:

$$\frac{\partial \xi}{\partial t} = \frac{G(\Theta) g(\xi)}{t_{c,\mathrm{ad}}}. \tag{4}$$

The parameter $t_{c,\mathrm{ad}}$ characterizes the time scale of crystallization. It is defined as $t_{c,\mathrm{ad}} = G_{c,\mathrm{ad}}/L_c$, where $G_{c,\mathrm{ad}}$ is the direction-averaged linear growth velocity of the

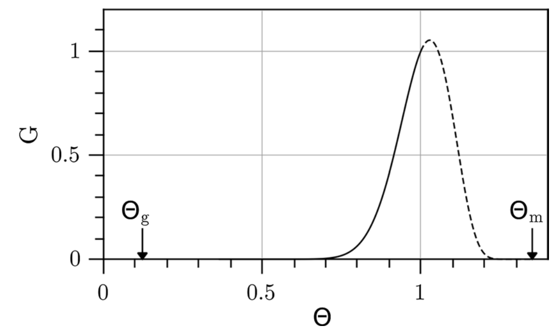

Fig. 2 Non-dimensional crystal growth velocity. $\Theta_{\mathrm{m}} = 1.349$; $\Theta_{\mathrm{g}} = 0.123$; $C_1 = 13.23$; $C_2 = 0.660$; $C_3 = 1.564$ (after [8])

crystals at the reference temperature T_{ad}, while L_c denotes the average distance between neighbouring nuclei. The function $G(\Theta)$ describes the strong temperature dependence of the crystal growth velocity, while the function $g(\xi)$ accounts for the mutual hindering of the growing crystals. A general procedure for determining the kinetic parameters and functions from measurements is provided in [4]; cf. also [17] for thermodynamic implications of the rate equations due to [4]. As in [8], the following functions are used in the present analysis:

$$g(\xi) = (9/2)^{1/3}(1-\xi)[-\ln(1-\xi)]^{2/3}; \tag{5}$$

$$G(\Theta) = \exp\left\{-\frac{C_1(1-\Theta)}{(1-\Theta_{\mathrm{g}})(\Theta-\Theta_{\mathrm{g}})} + C_2(C_3+\Theta_{\mathrm{m}})\left[\frac{1}{\Theta_{\mathrm{m}}-1} - \frac{C_3+1}{(C_3+\Theta)(\Theta_{\mathrm{m}}-\Theta)}\right]\right\}, \tag{6}$$

with

$$\Theta_{\mathrm{m}} = \frac{T_{\mathrm{m}} - T_S}{T_{\mathrm{ad}} - T_S} = \frac{c_{pL}(T_{\mathrm{m}} - T_S)}{l}; \quad \Theta_{\mathrm{g}} = \frac{T_{\mathrm{g}} - T_S}{T_{\mathrm{ad}} - T_S} = \frac{c_{pL}\left(T_{\mathrm{g}} - T_S\right)}{l}, \tag{7}$$

where T_{m} and T_{g} are the melting and the glass transition temperature, respectively. The non-dimensional parameters C_1 and C_2 are the activation energies for diffusion and nucleation, respectively, referred to the latent heat, while $C_3 = c_{pL} T_S / l$.[2] A typical example for $G(\Theta)$ is shown in Fig. 2, which is taken from [8] in order to allow comparison of the present analytical results with the previous numerical solutions. Since the temperature cannot exceed the temperature T_{ad}, the region $\Theta > 1$ is beyond reach for the crystallization process. That part of the graph can be

[2] An additional constant C_4 was introduced in [8], but it follows from the definitions that $C_4 = C_3 + 1$.

seen as a dashed line in Fig. 2. Note that with the parameter values of the particular example given in Fig. 2, the maximum growth rate is at a peak value Θ_p larger than 1, i.e. beyond reach in case of the parameters of Fig. 2. However, for another set of parameter values, peak values $\Theta_p \leq 1$ are possible.

4 Solution of the heat diffusion equation for the substrate

Heat conduction in the substrate is governed, of course, by the heat diffusion equation. Apart from initial conditions and boundary conditions at infinity, the solution of the heat diffusion equation for the substrate has to satisfy a coupling condition at the interface between the substrate and the crystallizing layer. If thermal contact resistance can be neglected, requiring the heat flux $\dot{q}_i$ to be continuous at the interface serves as the coupling condition.

In many cases of practical interest the thermal diffusivity of the substrate, α_S, is much smaller than the thermal diffusivity of the crystallizing layer, α_L. For a germanium film mounted on a quartz substrate, for example, the ratio α_S/α_L is about 0.16 [3]. Since the layer is very thin, α_L controls heat conduction in longitudinal, i.e. x-direction, whereas in the substrate heat conduction in lateral, i.e. y-direction, is characterized by α_S. Thus, if $\alpha_S \ll \alpha_L$, the penetration depth of the thermal disturbances in the substrate can be expected to be much smaller than the longitudinal extension of the temperature disturbances in the layer. It follows that the temperature gradient in the substrate will be mainly in y-direction, and a one-dimensional approximation of the heat diffusion equation will be sufficient to describe heat conduction in the substrate.

The solution for the substrate has to be coupled to the solution for the crystallizing layer. In view of (2) it is desirable to obtain an equation for the heat flux at the surface of the substrate in terms of the temperature at the surface. A convenient approach is to observe that not only the temperature T itself, but also the derivative with respect to y, denoted by T_y, has to satisfy the heat diffusion equation. Thus,

$$\frac{\partial T_y}{\partial t} = \alpha_S \frac{\partial^2 T_y}{\partial y^2}. \tag{8}$$

The problem is to be solved subject to the following initial and boundary conditions:

$$T - T_S = 0 \quad \text{at} \quad t = 0,\ y > 0; \tag{9}$$

$$T - T_S = \left(l/c_{pL}\right)\Theta(t;x) \quad \text{at} \quad y = 0, t > 0; \tag{10}$$

$$T - T_S = 0 \quad \text{as}\, y \to \infty. \tag{11}$$

Equations (9) and (11) imply that $T_y = 0$ for $t = 0, y > 0$ and for $y \to \infty$, respectively. Note that x serves as a parameter to the heat conduction problem of the substrate.

The solution can be found by applying Duhamel's integral formula, see [18], p. 327. With

$$-\frac{1}{\sqrt{\pi\alpha_S t}}\exp\left(-\frac{y^2}{4\alpha_S t}\right) \tag{12}$$

as the temperature response to a unit step-function change with time in the surface temperature, one obtains the solution

$$T_y(y,t;x) = -\frac{l}{c_{pL}\sqrt{\pi\alpha_S}}\frac{\partial}{\partial t}\int\limits_{0+}^{t}\frac{\Theta(\tau;x)}{\sqrt{t-\tau}}\exp\left[-\frac{y^2}{4\alpha_S(t-\tau)}\right]\mathrm{d}\tau. \tag{13}$$

5 Extended heat diffusion equation for the crystallizing layer

In the absence of thermal contact resistance, the heat flux at the surface of the substrate is equal to the interface heat flux. Evaluating (13) at the surface, $y = 0$, then gives the following integral representation of the interface heat flux:

$$\dot{q}_i = \frac{l\rho_S c_{pS}}{c_{pL}}\sqrt{\frac{\alpha_S}{\pi}}\frac{\partial}{\partial t}\int\limits_{0+}^{t}\frac{\Theta(\tau;x)}{\sqrt{t-\tau}}\mathrm{d}\tau. \tag{14}$$

The coupling of the equations for the crystallizing layer and the substrate, respectively, can now be accomplished by introducing (14) into (2), to obtain the following extended heat diffusion equation for the crystallizing layer:

$$\frac{\partial\Theta}{\partial t} - \alpha_L\frac{\partial^2\Theta}{\partial x^2} = \frac{\partial\xi}{\partial t} - \frac{1}{\delta_L}\frac{\rho_S c_{pS}}{\rho_L c_{pL}}\sqrt{\frac{\alpha_S}{\pi}}\frac{\partial}{\partial t}\int\limits_{0+}^{t}\frac{\Theta(\tau,x)}{\sqrt{t-\tau}}\mathrm{d}\tau. \tag{15}$$

According to the integral term of (15), the heat loss due to the presence of the substrate is not a local, instantaneous effect; it rather depends on the history of the process.

Together with the rate Eq. (4), the extended heat diffusion Eq. (15) forms a complete set of equations for the temperature of the layer and the degree of crystallization. The initial and boundary conditions depend on the particular process. An important example will be considered in the next section.

For a numerical solution, it may be convenient to integrate (15) over the time subject to the initial conditions

$$\Theta = \Theta_0(x), \xi = \xi_0(x) \text{ at } t = 0. \tag{16}$$

Introducing an auxiliary variable Ψ, one then obtains the following set of equations, which is equivalent to (15):

$$\frac{\partial \Psi}{\partial t} = \Theta; \tag{17}$$

$$\alpha_L \frac{\partial^2 \Psi}{\partial x^2} = \Theta - \Theta_0 - (\xi - \xi_0) + \frac{1}{\delta_L} \frac{\rho_S c_{pS}}{\rho_L c_{pL}} \sqrt{\frac{\alpha_S}{\pi}} \int_{0+}^{t} \frac{\Theta(\tau, x)}{\sqrt{t-\tau}} \mathrm{d}\tau, \tag{18}$$

with the additional initial condition

$$\Psi \equiv 0 \text{ at } t = 0. \tag{19}$$

6 Crystallization waves of invariant properties

6.1 Governing equations

Early numerical investigations of adiabatic layers [6] as well as more recent experiments with layers mounted on substrates [1, 11, 12] have shown that, under certain conditions, crystallization of amorphous materials may develop into a self-sustaining crystallization wave that propagates with invariant properties, in particular with constant velocity. In what follows, self-sustaining crystallization waves will be investigated as particular solutions of the set of equations given above.

With the aim of describing crystallization waves that propagate in negative x-direction with invariant properties, a non-dimensional wave coordinate η is introduced as

$$\eta = (U/\alpha_L)(x + Ut), \tag{20}$$

and the variables are assumed to depend on η only, i.e.,

$$\Theta = \Theta(\eta); \xi = \xi(\eta). \tag{21}$$

The propagation velocity U is a priory unknown and has to be determined as part of the solution, which has to satisfy the following boundary conditions far ahead and far behind the wave, respectively:

$$\Theta = 0, \xi = 0 \text{ as } \eta \to -\infty; \tag{22}$$

$$\Theta = 0 \text{ as } \eta \to +\infty. \tag{23}$$

Note that $\xi = 0$ far ahead of the wave implies that the substrate temperature is lower than the glass transition temperature. Otherwise, the amorphous material would start to crystallize before the wave arrives.

The variables according to (20) and (21) are introduced into the governing equations. The energy Eq. (15) can then be integrated once, making use of the boundary condition (22). Together with the rate Eq. (4) the final set of equations becomes:

$$\frac{\mathrm{d}\Theta}{\mathrm{d}\eta} = \Theta - \xi + \frac{1}{\sqrt{\pi}} H\lambda \int_{-\infty}^{\eta} \frac{\Theta(s)}{\sqrt{\eta - s}} \mathrm{d}s; \tag{24}$$

$$\frac{\mathrm{d}\xi}{\mathrm{d}\eta} = \lambda^2 G(\Theta) g(\xi), \tag{25}$$

where the non-dimensional parameters

$$H = \frac{\rho_S c_{pS}}{\rho_L c_{pL}} \frac{\sqrt{\alpha_S t_{c,\mathrm{ad}}}}{\delta_L} \tag{26}$$

and

$$\lambda = \frac{1}{U} \sqrt{\frac{\alpha_L}{t_{c,\mathrm{ad}}}} \tag{27}$$

have been introduced. While λ represents a non-dimensional inverse of the propagation speed, the parameter H characterizes the heat loss due to the contact of the crystallizing layer with the substrate. Since the integro-differential Eq. (24) and the differential Eq. (25) as well as the boundary conditions (22) and (23) are homogeneous, λ plays the role of an eigenvalue. When λ has been determined as part of the solution of the eigenvalue problem, the propagation speed can be obtained from (27).

The set of Eqs. (24)–(27) is in agreement with the corresponding equations derived in [8, 9] on a different way. The method of solution will also be different. While numerical solutions were given in [8, 9], an asymptotic expansion will be performed in what follows, with the aim of obtaining analytical solutions.

6.2 Solution for large activation energy of molecular diffusion

For most amorphous materials that are of interest with regard to explosive crystallization, the activation energy for molecular diffusion is much larger than the activation energy for nucleation. Germanium and other semiconductors provide examples [3]. In the present notation, cf. Section 3.2, this leads to $C_1 \gg 1$, while $C_2 = \mathrm{O}(1)$ and $C_3 = \mathrm{O}(1)$. The values of the parameters C_1 to C_3 as given in the caption to Fig. 2 for a particular example reflect that general behaviour.

As in [8, 9], the present analysis will be restricted to the case $\Theta_\mathrm{p} > 1$, i.e. the maximum of the crystal growth velocity is not attained in the crystallization process, cf. Figure 2. In this case, estimates of the orders of magnitudes indicate that three zones of the crystallization wave can be distinguished. The first zone is a preheating zone, in which crystallization is negligible, but the heat loss into the substrate is substantial. When a sufficiently high temperature has been reached, substantial crystallization sets in to form a very thin crystallization zone with negligible heat loss. After crystallization has been completed, the process is terminated in a cooling zone of large length. The following application of the method of matched asymptotic expansions for $C_1 \to \infty$ will show that the assumed structure of the wave is correct, provided the condition $\Theta_p > 1$ is satisfied. If $\Theta_p \le 1$, however, more complicated structures of crystallization waves have been found with numerical solutions [3].

6.2.1 Preheating zone

It is easy to check that

$$\Theta = \Theta_g \exp(K\eta) \tag{28}$$

is a solution of the integro-differential Eq. (24) with $\xi \equiv 0$, if the constant K satisfies the equation

$$(K-1)\sqrt{K} = H\lambda. \tag{29}$$

According to (28), the origin of the η-coordinate has been chosen such that $\eta = 0$ for $\Theta = \Theta_g$. An exact solution of (29) can be found in [8]. However, it will turn out that only very small values of $H\lambda$ will be of relevance for the further analysis. Thus, the solution

$$K = 1 + H\lambda + \ldots \quad \text{for } H\lambda \ll 1 \tag{30}$$

will be used in what follows.

Concerning matching the preheating zone with the crystallization zone, it is to be taken into account that the total amount of latent heat liberated in the crystallization zone has to be conducted forward, as the temperature gradient in the cooling zone will turn out to be too small to make a substantial contribution. This gives the following matching condition in terms of non-dimensional variables:

$$\frac{d\Theta}{d\eta} = 1 \text{ as } \eta \to \eta^*, \tag{31}$$

with η^* as the η-coordinate of the very thin crystallization zone. Inserting (28) gives

$$\eta^* = -(1/K)\ln\left(K\Theta_g\right) = -\ln\Theta_g + H\lambda\left(\ln\Theta_g - 1\right) + \ldots; \tag{32}$$

$$\Theta^* = 1/K = 1 - H\lambda + \ldots, \tag{33}$$

where $\Theta^* = \Theta(\eta^*)$. The dots in Eqs. (32) and (33) stand for higher-order terms in an expansion for $H\lambda \ll 1$.

6.2.2 Crystallization zone

In order to obtain equations that, on the one hand, are free of the expansion parameter C_1 and, on the other hand, allow matching between the crystallization zone and the preheating zone, the following stretched variables and parameters are introduced:

$$\tilde{\eta} = C_1\left(1-\Theta_g\right)^{-2}\left(\eta - \eta^*\right); \tilde{\Theta} = C_1\left(1-\Theta_g\right)^{-2}\left(\Theta - \Theta^*\right); \tag{34}$$

$$\tilde{H} = C_1^{3/2}\left(1-\Theta_g\right)^{-3}H; \tilde{\lambda} = C_1^{-1/2}\left(1-\Theta_g\right)\lambda; \tag{35}$$

i.e. crystallization takes place in very thin layer near $\eta = \eta^*$ and a very small temperature regime near $\Theta = \Theta^*$. The coefficients containing $\left(1-\Theta_g\right)$ have been introduced in order to obtain the final results as universal relationships.

Introducing (34) and (35) into the governing Eqs. (24) and (25) with $G(\Theta)$ according to (6), and expanding for $C_1 \to \infty$, one obtains in first order the following set of equations:

$$\frac{d\tilde{\Theta}}{d\tilde{\eta}} = 1 - \xi; \tag{36}$$

$$\frac{d\xi}{d\tilde{\eta}} = \tilde{\lambda}^2 G\left(\tilde{\Theta}\right) g(\xi), \tag{37}$$

with

$$G\left(\tilde{\Theta}\right) = \exp(\tilde{\Theta} - \tilde{H}\tilde{\lambda}), \tag{38}$$

whereas $g(\xi)$ remains unchanged as given in (5).

For solving the above set of equations it is convenient to eliminate the coordinate $\tilde{\eta}$ by taking the quotient of (37) and (36), i.e. considering the process in the phase plane $\left(\xi, \tilde{\Theta}\right)$. This gives

$$\frac{d\xi}{d\tilde{\Theta}} = (9/2)^{1/3}\tilde{\lambda}^2 G\left(\tilde{\Theta}\right)[-\ln(1-\xi)]^{2/3}, \tag{39}$$

with the boundary (matching) conditions

$$\xi = 0 \text{ as } \tilde{\Theta} \to -\infty; \tag{40}$$

$$\xi = 1 \text{ as } \tilde{\Theta} \to 0. \tag{41}$$

As there are two boundary conditions for a differential equation of first order, the Eqs. (39), (40) and (41) form an eigenvalue problem, with $\tilde{\lambda}$ being the eigenvalue. The solution can be found by separating the variables in (39) and integrating. Observing the boundary condition (40), one obtains

$$\gamma\left(\frac{1}{3}, z\right) = \left(\frac{9}{2}\right)^{\frac{1}{3}} \tilde{\lambda}^2 \exp(\tilde{\Theta} - \tilde{H}\tilde{\lambda}), z = -\ln(1-\xi), \tag{42}$$

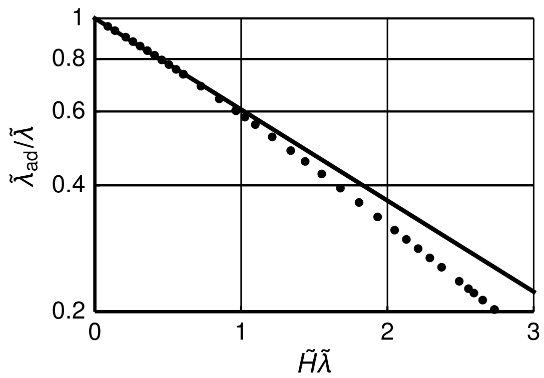

Fig. 3 Propagation velocity, referred to the adiabatic propagation velocity, $\tilde{\lambda}_{ad}/\tilde{\lambda}$, as a function of the combined heat loss parameter $\tilde{H}\tilde{\lambda}$. *Solid line* Universal analytical result according to (43). *Dots* numerical results for λ_{ad}/λ with the parameter set given in the caption to Fig. 2 [8]

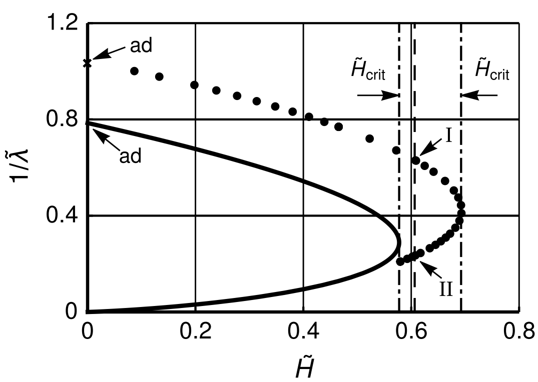

Fig. 4 Non-dimensional propagation velocity $1/\tilde{\lambda}$ as a function of the heat loss parameter $\tilde{H}$. *Solid line* universal analytical result according to (44) and (45). *Dots* numerical results for the parameter set given in the caption to Fig. 2 [8]

where γ the incomplete Gamma function; cf. [19], p. 260. The eigenvalue is then obtained by accounting also for the boundary condition (41). This gives

$$\tilde{\lambda} = \tilde{\lambda}_{ad}\exp\left(\tilde{H}\tilde{\lambda}/2\right), \tag{43}$$

see Fig. 3, where

$$\tilde{\lambda}_{ad} = \left(\frac{2}{9}\right)^{\frac{1}{6}}\sqrt{\Gamma\left(\frac{1}{3}\right)} \tag{44}$$

is the eigenvalue for the adiabatic case, i.e. in the absence of a substrate. Γ is the Gamma function; cf. [19], pp. 255. Equation (44) is in accord with the result given in [2] for the "subcritical wave".

The exponential function in (43) shows that the effect of the heat loss on the eigenvalue is characterized not solely by the heat loss parameter, but rather by the product of the heat loss parameter and the eigenvalue itself. However, in most applications the heat loss parameter $\tilde{H}$ will be given and the eigenvalue $\tilde{\lambda}$ is to be determined. Thus, the implicit Eq. (43) for the eigenvalue is re-written in the more convenient explicit form

$$\tilde{H} = \left(2/\tilde{\lambda}\right)\ln\left(\tilde{\lambda}/\tilde{\lambda}_{ad}\right). \tag{45}$$

This equation shows two interesting properties of the solution; cf. Fig. 4. First, a (real) solution exists only if the heat loss parameter is below a critical value, which is obtained as

$$\tilde{H}_{crit} = 2/\tilde{\lambda}_{crit}, \tag{46}$$

with the critical eigenvalue

$$\tilde{\lambda}_{crit} = \mathrm{e}\,\tilde{\lambda}_{ad}. \tag{47}$$

Secondly, for $\tilde{H} < \tilde{H}_{crit}$, there are two branches of the solution, i.e., two eigenvalues are associated with one heat loss parameter. This will be further discussed in Sect. 7.

Equation (42) is a relation between temperature and degree of crystallization. The dependence of those variables on the wave coordinate can be obtained by integrating (36) or (37). It is easy to see that $\tilde{\eta} \to -\infty$ as $\xi \to 0$, and $\tilde{\eta} \to +\infty$ as $\xi \to 1$, as required by the conditions of matching to the preheating zone and the cooling zone, respectively.

6.2.3 Cooling zone

Under the present assumptions, crystallization is completed in the crystallization zone. Thus, $\xi \equiv 1$ in the cooling zone. The length of the cooling zone was estimated previously [8] to be of the order of $(H\lambda)^{-2}$, i.e. of the order of C_1^2 in terms of the large parameter of the present asymptotic expansion, see (35). Therefore, the stretched length coordinate

$$\hat{\eta} = \left(\eta - \eta^*\right)/C_1^2 \tag{48}$$

is introduced to describe the temperature distribution $\Theta = \hat{\Theta}\left(\hat{\eta}\right)$ in the cooling zone. With (35), (48), $\xi \equiv 1$ and an expansion for large C_1, the energy Eq. (24) reduces to

$$\hat{\Theta}\left(\hat{\eta}\right) + \Lambda\int_0^{\hat{\eta}} \frac{\hat{\Theta}\left(\hat{s}\right)}{\sqrt{\hat{\eta} - \hat{s}}}\mathrm{d}\hat{s} = 1, \tag{49}$$

with

$$\Lambda = \left(1 - \Theta_g\right)^2\tilde{H}\tilde{\lambda}/\sqrt{\pi}. \tag{50}$$

(49) is an Abel integral equation of the second kind. A solution can be found according to [20], p. 138. Using known properties of the Gamma functions [19], pp. 255–260, one obtains

$$\hat{\Theta} = -2\Lambda\sqrt{\hat{\eta}} + e^{\zeta}\left[1 - (2/\sqrt{\pi})\gamma\left(\frac{3}{2},\zeta\right)\right], \zeta = \pi\Lambda^2\hat{\eta}. \quad (51)$$

It may be of interest to know how the temperature decays as $\hat{\eta} \to \infty$. With an asymptotic expansion of the incomplete Gamma function, see [19], p. 263, (51) gives

$$\hat{\Theta} = 1/\pi\Lambda\sqrt{\hat{\eta}} \text{ as } \hat{\eta} \to \infty; \quad (52)$$

or, with (50), (48) and (35),

$$\Theta = 1/H\lambda\sqrt{\pi\eta} \text{ as } \eta \to \infty. \quad (53)$$

(53) is in accord with the result derived previously by other means [3] and quoted already in [8].

It ought to be noted that the solution (51) exhibits a shortcoming. As $\hat{\eta} \to 0$, $\mathrm{d}\hat{\Theta}/\mathrm{d}\hat{\eta} \to -\Lambda/\sqrt{\hat{\eta}} \to -\infty$. Since the same singular behavior of the first derivative of the temperature can also be obtained directly from the integral Eq. (49), (49) itself is not uniformly valid. In the framework of matched asymptotic expansions, a small subzone near $\hat{\eta} = 0$, perhaps even more than one subzone, would have to be introduced to deal with that non-uniformity. A more direct approach could be to take the whole integral of (24) into account, i.e., add in (49) the missing part of the integral in order to obtain a smooth transition from the crystallization zone to the cooling zone. It turned out, however, that the solution of the resulting Abel integral equation of the second kind could not be found in closed form. Since the solution for the cooling zone affects neither the propagation velocity nor the distribution of the degree of crystallization, we refrain from dealing with those details of the cooling zone.

6.3 Comparison with numerical solutions and experimental data

Numerical solutions of the present problem for a particular set of kinetic and thermodynamic parameters are available in [8]. Regrettably, excellent agreement between those numerical results and the present asymptotic solutions cannot be expected for at least two reasons. First, the particular value of the non-dimensional activation energy C_1, which is appropriate for polymers, is only about 13, implying an error of the order of 10 to 20%. It is true that semiconductors would provide larger values of C_1, cf. below, but there is a lack of data for heterogeneous crystallization of semiconductors [3]. Secondly, Fig. 2 shows that the adiabatic end temperature is rather close to the peak temperature, where the asymptotic expansion that leads to a linear approximation of the temperature in the crystallization zone, cf. (38), ceases to be valid. This will have a rather strong effect on the adiabatic case, which may indirectly also affect the results that account for the substrate.

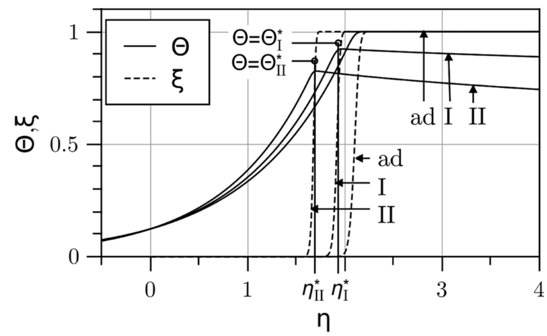

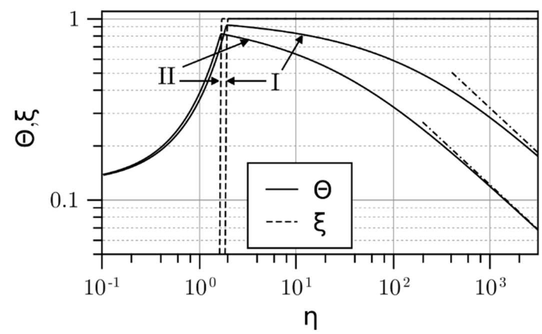

Fig. 5 Non-dimensional temperature Θ and degree of crystallization ξ as functions of the longitudinal wave coordinate η. Numerical solutions [8] for the parameter set given in the caption to Fig. 2. *ad* adiabatic (no substrate), I and II… $H = 0.0085$; I… upper branch, II… lower branch in Fig. 3. *Upper diagram*: linear scales; analytical solutions $\eta_{\mathrm{I}}^* \approx 1.93$, $\eta_{\mathrm{II}}^* \approx 1.69$ and $\Theta_{\mathrm{I}}^* \approx 0.95$, $\Theta_{\mathrm{II}}^* \approx 0.87$ according to (32) and (33), respectively. *Lower diagram*: double log scales. *Dashed-dotted line*: asymptote according to (53)

Subject to those reservations, comparisons of numerical results with analytical solutions for the propagation velocity are shown in Figs. 3 and 4. In Fig. 3, the propagation velocity is referred to the value for the adiabatic process. Thus, the effect of the substrate on the propagation velocity is visible in Fig. 3 as the dependence of $\tilde{\lambda}_{\mathrm{ad}}/\tilde{\lambda}$ on the combined parameter $\tilde{H}\tilde{\lambda}$. Note that, according to the definitions (35), (26) and (27), $\tilde{H}\tilde{\lambda}$ is free of the kinetic parameter $t_{c,\mathrm{ad}}$, which characterizes the time scale of crystallization. Since $\tilde{\lambda}$ is normally not known a priori, Fig. 4 will be more convenient when the propagation velocity ought to be determined for a given heat loss parameter $\tilde{H}$. It may appear surprising that the agreement between the analytical solution and the numerical results is less good in Fig. 4 than in Fig. 3. This is because the diagram of Fig. 4, in contrast to Fig. 3, is directly affected by the propagation velocity for the adiabatic process, which is not very well approximated for the reasons given above.

Of particular interest are the critical values. Concerning the eigenvalues, (47) gives the universal relationship $\tilde{\lambda}_{\text{crit}}/\tilde{\lambda}_{\text{ad}} = \text{e} \approx 2.72$, which is to be compared with the numerical result $\tilde{\lambda}_{\text{crit}}/\tilde{\lambda}_{\text{ad}} \approx 2.5$. For the critical value of the heat loss parameter, one obtains from (46) together with (35), (44) and the parameter set given in the caption to Fig. 2 the value $H_{\text{crit}} = 8.1 \times 10^{-3}$, whereas the value obtained from the numerical solution [8] is $H_{\text{crit}} \approx 9.7 \times 10^{-3}$.

Furthermore, the position and the temperature of the crystallization zone are considered. Figure 5 shows the numerical results for $H = 0.0085$ [8]. According to [8], there are two solutions for $H = 0.0085$, with the numerical eigenvalues $\lambda_{\text{I}} \approx (0.16)^{-1}$ and $\lambda_{\text{II}} \approx (0.065)^{-1}$, respectively. As can be seen in Fig. 4, those numerical values are out of reach for the analytical solution. Thus, the eigenvalues λ_{I} and λ_{II} are taken from the numerical results and introduced into the analytical solutions (32) and (33). This gives $\eta_{\text{I}}^* \approx 1.93$, $\eta_{\text{II}}^* \approx 1.69$ and $\Theta_{\text{I}}^* \approx 0.95$, $\Theta_{\text{II}}^* \approx 0.87$, respectively. As can be seen in the upper diagram of Fig. 5, the analytic results are in good agreement with the numerical solutions.

Finally, the relation (53) for the cooling region is tested by numerical means. The lower diagram of Fig. 5 shows that (53) provides precisely the asymptote to the numerical solution. In addition, it is easy to recognize the three different zones in the two diagrams of Fig. 5.

Concerning measurements, one may consult [3], where data for germanium layers on quartz substrates are collected. With the data given in Table 1 and Fig. 2 of [3], one obtains (in the present notation): $\alpha_L = 7.3 \times 10^{-6}\,\text{m}^2/\text{s}$, $l/c_{pL} = T_{\text{ad}} - T_S = 477\,\text{K}$, $C_1 \approx 56$, $T_p \approx 940\,\text{K}$. The lowest substrate temperature in the experiments [1], as quoted in [3], is $T_S \approx 620\,\text{K}$. Thus, the adiabatic end temperature T_{ad} is above the peak temperature, and the present analysis cannot be applied to obtain quantitative comparisons. One may expect, however, that in this case, crystallization takes place mainly at temperatures close to the peak temperature. As far as the adiabatic process, is concerned an asymptotic analysis has indeed confirmed that expectation [2]. Thus, the time scale of crystallization will correspond to the maximum growth rate, i.e., $t_c \sim \left(G_C^3 I_C\right)^{-1/4} \sim 10^{-7}\,\text{s}$ according to Fig. 2 of [3]. Furthermore, according to [3], $T_S \approx 620\,\text{K}$ leads to a value of H close to the critical value of H, which reduces the propagation velocity U by a factor of about e^{-1}, cf. (47), as compared to the adiabatic value. The latter may be estimated with (44), but, as $T_{\text{ad}} > T_p$ in this case, a better estimate can be obtained from Eq. (185) of [2]; it reads $U_{\text{ad}} \sim C_1^{-3/8}\sqrt{\alpha_L/t_c} \approx 1.9\,\text{m/s}$. After division by e one obtains $U \sim 0.7\,\text{m/s}$. That value is between the two values measured for $T_S \approx 620\,\text{K}$ [1, 3], making the estimate appear satisfactory.

7 Conclusions and discussion

The present analysis of explosive crystallization is based on first principles. The energy equation of the crystallizing layer is coupled, on the one hand, to a rate equation of crystallization and, on the other hand, to a solution of the heat diffusion equation for the substrate. The rate equation was derived previously [4] from a theory of non-isothermal crystallization that accounts for all essential physical phenomena [13–16]. The use of semi-empirical laws as in [21–24], for instance, is thereby avoided. The heat diffusion equation is solved by applying Duhamel's integral. The result shows that the heat loss from the layer due to the presence of the substrate depends on the history of the process. This is in contrast to descriptions with an apparent heat transfer coefficient [22–25].

For explosive crystallization fronts that propagate as waves with invariant properties, the governing equations can be transformed to a set of equations consisting of an integro-differential equation and an ordinary differential equation. In previous work [8, 9], those equations were solved numerically for a particular set of non-dimensional parameters. In the present work, however, an asymptotic analysis is given. It provides results that are exact in the limit $C_1 \rightarrow \infty$, where C_1 is the activation energy of molecular diffusion referred to the latent heat; cf. [8]. The asymptotic solutions can serve as approximations for applications of practical interest.

An important quantity in the description of the crystallization process is the linear growth velocity of the crystals. Based on thermodynamic considerations, the crystal growth velocity as a function of temperature is required to have a maximum at a certain peak temperature, where the activation of nuclei due to sub-cooling and the hindering due to molecular diffusion balance each other. Strictly speaking, the present analysis is applicable only to temperatures below the peak temperature. However, only the non-dimensional activation energy of diffusion appears in the first-order results of the asymptotic analysis, whereas the contribution of the activation energy of nuclei turned out to be negligible. Thus, the present results are also valid if the growth velocity is simply modelled with an exponential function of the Arrhenius type, as it is often done [22, 23, 26–34].

According to the present asymptotic analysis, the crystallization wave consists of three zones. In the preheating zone, the temperature of the amorphous material is elevated up to the point where crystallization becomes noticeable. Crystallization is completed in the crystallization zone, which occupies only a very small temperature interval. The crystallization zone is followed by the large cooling zone, where the temperature of the fully crystallized layer decays due to the conduction of heat into the substrate. It is remarkable that the cooling zone does not affect the propagation velocity of the crystallization wave.

Written in the reduced non-dimensional quantities labelled by a tilde in the equations given above, the results of the analysis are "universal" in the sense that they comprise the influence of all non-dimensional parameters that govern the process. As far as the orders of magnitude in terms of the large parameter C_1 are concerned, the effective heat loss parameter $\tilde{H}$ turned out to be of the order of $C_1^{3/2}H$, i.e., much larger than one might have expected in view of the appearance of the heat loss parameter H in the energy equation of the layer. On the other hand, the propagation velocity U is of the order of $\sqrt{\alpha_L/t_{c,\mathrm{ad}}C_1}$, i.e., much smaller than the reference velocity $\sqrt{\alpha_L/t_{c,\mathrm{ad}}}$ appearing in (27).

Of particular interest for applications is the critical value of the heat loss parameter. The non-dimensional results given above can be re-written in dimensional quantities to obtain the following condition for the existence of crystallization waves that propagate with invariant properties:

$$\frac{\delta_L}{\sqrt{\rho_S c_{pS} k_S}}\left[1-\frac{c_{pL}\left(T_g-T_S\right)}{l}\right]^3 \geq \frac{\mathrm{e}}{2^{5/6}9^{1/6}}\frac{C_1^{3/2}}{\rho_L c_{pL}}\sqrt{\Gamma\left(\frac{1}{3}\right)t_{c,\mathrm{ad}}}, \tag{54}$$

where the thermal conductivity of the substrate, k_S, has been introduced for convenience. On the right-hand side of (54) there are only thermodynamic and kinetic quantities of the crystallizing layer, whereas all parameters characterizing the substrate have been collected on the left-hand side. This allows the following conclusions with regard to the existence of crystallization waves that propagate with invariant properties:

- If all material properties and the substrate temperature are fixed, the thickness of the layer must not be too small. This is in accord with observations [26, 31, 35, 36].
- If all material properties and the layer thickness are fixed, the substrate temperature must not be too small. This is also in accord with observations [1].
- If the material properties of the layer, the thickness of the layer and the temperature of the substrate are fixed, the material properties of the substrate must be such that $\rho_S c_{pS} k_S$ is not too large. This was already mentioned in [8].

If the inequality of (54) is satisfied, two solutions are found to exist for one and the same value of the heat loss parameter. Of course, the existence of dual solution raises the question of the stability of the solutions. The experimental data given in [1] suggest that the solution with the larger propagation velocity for a given heat loss parameter, i.e. the upper branch in Fig. 4, is stable, whereas the other one may be unstable. Difficulties with the numerical solutions [3, 8] point into the same direction. A thorough investigation of various instabilities, cf. [37–42], is certainly desirable.

The present analysis as well as previous theoretical work, e.g. [3], have revealed a lack of kinetic data for the crystallization of amorphous materials that are of practical relevance. Future investigations based on comparisons of theoretical results with available experimental data, perhaps following the way proposed in [4], might help to fill that gap.

Finally it should be noted that an analysis based on rate equations, such as [3, 8] and the present one, may provide a basis for a variety of generalizations, see [17, 43–51] for examples.

Acknowledgements Open access funding provided by TU Wien (TUW). The author should like to thank his former collaborator Dr. Christoph Buchner, presently with FOTEC Forschungs- und Technologietransfer GmbH, Wiener Neustadt, Austria, for many fruitful discussions when this work was in progress. Dr. Buchner also found, and eliminated, an error in the first version of the analysis and provided the numerical results. Furthermore, the author is grateful Prof. G. Eder, Linz, for valuable comments and to Dr. Markus Müllner for his help in preparing the figures. Financial support by Androsch International Management Consulting GmbH, Vienna, is also gratefully acknowledged.

References

1. Grigoropoulos C, Rogers M, Ko SH, Golovin AA, Matkowsky BJ (2006) Explosive crystallization in the presence of melting. Phys Rev B 73:184125
2. Köppl A (1990) Anwendung von Ratengleichungen auf anisotherme Kristallisation von Kunststoffen. Dissertation, Technical University of Vienna, Vienna, Austria
3. Buchner C, Schneider W (2015) Explosive crystallization in thin amorphous layers on heat conducting substrates. J Appl Phys 117:245301
4. Schneider W, Köppl A, Berger J (1988) Non-isothermal crystallization of polymers—system of rate equations. Int Polym Process 2(3/4):151–154
5. Köppl A, Schneider W, Berger J (1987) Ausbreitungsgeschwindigkeit und Struktur von Kristallisationswellen. GAMM Annual Meeting, Stuttgart, Germany
6. Berger J (1988) Erstarren von Kunststoffen unter dem Einfluß von Wärmeleitung und Kristallisationskinetik. Dissertation, Technical University of Vienna, Vienna, Austria

7. Schneider W, Berger J, Köppl A (1992) Non-isothermal crystallization of polymers: application of rate equations. In: Güçeri SI (ed), Proceedings of 1st international conference transport phenomena in processing. Technomic Publ., pp 1043–1054
8. Buchner C, Schneider W (2010) Explosive crystallization in thin amorphous layers on heat conducting substrates. In: Proceedings of international heat transfer conference (IHTC14). ASME, Washington, pp 275–284
9. Buchner C, Schneider W (2010) Crystallization waves in thin amorphous layers on heat conducting substrates. PAMM Proc Appl Math Mech 10:493–494
10. Buchner C, Schneider W (2014) Explosive-crystallization waves in thin amorphous layers on heat conducting substrates with thermal contact resistance. PAMM Proc Appl Math Mech 14:711–712
11. Ohdaira K, Fujiwara T, Endo Y, Nishizaki S, Matsumura H (2009) Explosive crystallization of amorphous silicon films by flash lamp annealing. J Appl Phys 106:044907
12. Rogers M, Ko SH, Grigoropoulos C (2006) In situ crystal growth imaging during explosive crystallization. In: Okada T et al. (eds) Proceedings of photon processing in microelectronics and photonics, vol V. 6106 of SPIE, paper number 610614, pp 610614-1–610614-8
13. Kolmogorov AN (1937) On the statistical theory of the crystallization of metals (in Russian). Izv Acad Nauk SSSR Math Ser 1:355–359
14. Avrami M (1939) Kinetics of phase change I. J Chem Phys 7:1103–1112
15. Avrami M (1940) Kinetics of phase change II. J Chem Phys 8:212–224
16. Avrami M (1941) Kinetics of phase change III. J Chem Phys 9:177–184
17. Hütter M (2001) Thermodynamically consistent in-corporation of the Schneider rate equations into two-phase models. Phys Rev E 64(011209):1–11
18. Korn GA, Korn TM (eds) (1968) Mathematical handbook for scientists and engineers, 2nd edn. McGraw-Hill, New York
19. Abramowitz M, Stegun IA (eds) (1965) Handbook of mathematical functions. Dover Publ, New York
20. Polyanin AD, Manzhirov AV (2008) Handbook of integral equations, 2nd edn. Chapman & Hall/CRC, Boca Raton
21. Germain P, Zellama K, Squelard S, Bourgoin JC, Gheorghiu A (1979) Crystallization in amorphous germanium. J Appl Phys 50:6986–6994
22. Heinig KH, Geiler H-D (1985) Phenomenological theory of explosive solid phase crystallization of amorphous silicon. I. Stationary solutions. Phys Stat Sol (a) 92:421–430
23. Heinig KH, Geiler H-D (1986) Phenomenological theory of explosive solid phase crystallization of amorphous silicon. II. Dynamical processes. Phys Stat Sol (a) 93:99–104
24. Geiler H-D, Glaser E, Götz G, Wagner M (1986) Explosive crystallization in silicon. J Appl Phys 59:3091–3099
25. Gilmer GH, Leamy HJ (1980) An analysis of the explosive crystallization of amorphous layers. In: White CS, Peercy PS (eds) Laser and electron beam processing of materials. Academic Press, Cambridge, pp 227–233
26. Götzberger A (1955) Über die Kristallisation aufgedampfter Antimonschichten. Z Physik 142:182–200
27. Knapp JA, Picraux ST (1981) Microsecond time-scale Si regrowth using a line-source electron beam. Appl Phys Lett 38:873–875
28. Köster U, Herold U (1981) Crystallization of metallic glasses. In: Güntherodt H-J, Beck H (eds) Glassy metals I, topics in applied physics, vol 46. Springer, Berlin, pp 225–259
29. Donovan EP, Spaepen F, Umemoto S, Poate JM, Jacobson DC (1983) Heat of crystallization and melting point of amorphous silicon. Appl Phys Lett 42:698–700
30. Olson GL, Roth JA (1988) Kinetics of solid phase crystallization in amorphous silicon. Mater Sci Rep 3:1–77
31. Shklovskii VA, Kuz'menko VM (1989) Explosive crystallization of amorphous substances. Sov Phys Usp 32:163–180
32. Farjas J, Roura P (2006) Modification of the Kolmogorov–Johnson–Mehl–Avrami rate equation for non-isothermal experiments and its analytical solution. Acta Mater 54:5573–5579
33. Johnson B, Gortmaker P, McCallum J (2008) Intrinsic and dopant-enhanced solid-phase epitaxy in amorphous germanium. Phys Rev B 77:214109
34. Sontheimer T, Becker C, Bloeck U, Gall S, Rech B (2009) Crystallization kinetics in electron-beam evaporated amorphous silicon on ZnO:Al-coated glass for thin film solar cells. Appl Phys Lett 95:101902
35. Takamori T, Messier R, Roy R (1972) New noncrystalline germanium which crystallizes 'explosively' at room temperature. Appl Phys Lett 20:201–203
36. Koba R, Wickersham CE (1982) Temperature and thickness effects on the explosive crystallization of amorphous germanium films. Appl Phys Lett 40: 672–675. Erratum: Appl Phys Lett 42: 398
37. van Saarloos W, Weeks JD (1983) Surface undulations in explosive crystallization: a thermal instability. Phys Rev Lett 51:1046–1049
38. Kurtze DA, van Saarloos W, Weeks JD (1984) Front propagation in self-sustained and laser-driven explosive crystal growth: stability analysis and morphological aspects. Phys Rev B 30:1398–1415
39. Shklovskij VA, Ostoushko VN (1996) Nonlinear resonance study of the periodic motion of the explosive crystallization front in glasses. Phys Rev B 53:3095–3106
40. Provatas N, Grant M, Elder KR (1996) Phase-field model for activated reaction fronts. Phys Rev B 53:6263–6272
41. Frankel M, Gross LK, Roytburd V (2000) Thermo-kinetically controlled pattern selection. Interfaces Free Bound 2:313–330
42. Smagin I, Nepomnyashchy A (2009) Stability analysis of explosive crystallization front in ESPE mode. Phys D 238:706–723
43. Andreucci D, Fasano A, Primicerio M, Ricci R (1996) Mathematical problems in polymer crystallization. Surv Math Ind 6:7–20
44. Eder G (1997) Fundamentals of structure formation in crystallizing polymers. In: Natada K et al (eds) Macromolecular design of polymeric materials. Marcel Dekker, Basel, pp 761–782
45. Eder G, Janeschitz-Kriegl H (1997) Crystallization. In: Meijer HEH (ed) Processing of polymers, material science and technology, vol 18. VCH, Weinheim, pp 270–342
46. Zuidema H, Peters GWM, Meijer HEH (2001) Influence of cooling rate on pVT-data of semicrystalline polymers. J Appl Polym Sci 82:1170–1186
47. Burger M, Capasso V, Micheletti A (2004) Optimal control of polymer morphologies. J Eng Math 49:339–358
48. Tanner RI, Qi F (2005) A comparison of some models for describing polymer crystallization at low deformation rates. J Non-Newtonian Fluid Mech 127:131–141
49. De Santis F, Lamberti G, Peters GWM, Brucato V (2005) Improved experimental characterization of crystallization kinetics. Eur Polym J 41:2297–2302
50. Janeschitz-Kriegl H (2010) Crystallization modalities in polymer melt processing. Springer, New York
51. Lee Wo D, Tanner RI, Fletcher DF (2012) A numerical treatment of crystallization in tube flow. Polym Eng Sci 52:1356–1366